N87-23325

# ANOMALOUS TRANSPORT IN DISCRETE ARCS AND SIMULATION OF DOUBLE LAYERS IN A MODEL AURORAL CIRCUIT

Robert A. Smith
Plasma Physics Division
Science Applications International Corporation
McLean, Virginia 22102, U.S.A.

## ABSTRACT

The evolution and long-time stability of a double layer (DL) in a discrete auroral arc requires that the parallel current in the arc, which may be considered uniform at the source, be diverted within the arc to charge the flanks of the U-shaped double layer potential structure. A simple model is presented in which this current redistribution is effected by anomalous transport based on electrostatic lower hybrid waves driven by the flank structure itself. This process provides the limiting constraint on the double layer potential. The flank charging may be represented as that of a nonlinear transmission line. A simplified model circuit, in which the transmission line is represented by a nonlinear impedance in parallel with a variable resistor, is incorporated in a one-dimensional simulation model to give the current density at the DL boundaries. Results are presented for the scaling of the DL potential as a function of the width of the arc and the saturation efficiency of the lower hybrid instability mechanism.

## I. INTRODUCTION

A vast body of ground-based, rocket, and satellite observations reveals that auroral-zone acceleration processes occur in a hierarchy of latitudinal scale widths. On the scale of the inverted-V region ($\Delta\Lambda > 1°$) parallel electric fields are observed in narrow, soliton-like structures interpreted as weak or ion-acoustic double layers (DL's) (Temerin et al., 1982). Assuming statistical homogeneity of the distribution of these weak DL's over an altitude range comparable to 1 $R_e$, one infers a total potential drop of up to a few kV, typical of the inverted-V region. On smaller spatial scales ($\Delta\Lambda < 0.1°$) more energetic precipitation is observed in discrete arcs, which have projected widths $\sim$1 km in the ionosphere. Discrete arcs (DA's) are associated with electrostatic shocks (Torbert and Mozer, 1978; Kletzing et al., 1983). We adopt the hypothesis that electrostatic shocks constitute the nearly field-aligned "flanks" of the paradigmatic U-shaped potential structure of a strong double layer. Although this hypothesis seems plausible, many questions exist concerning the conditions under which DL's may exist in space, their dynamics, and their structure. These questions are vital for understanding the complex observational morphology of fields and particles in the auroral zone. At present, investigations of such questions must to a large extent be motivated by and proceed from consideration of the fast-growing literature on experiments and simulations, although usually the applicability of these situations to DL's in space is indirect (Smith, 1985, 1986a).

In this paper, we first discuss theoretically the question of what limits the potential of DL's in auroral arcs, and report results of recent simulations of DL's in a model circuit. Somewhat more detailed expositions are given by Smith (1986b, c).

## II. THEORY

Experiments and simulations (Goertz and Joyce, 1975; Coakley and Hershkowitz, 1979) reveal a scaling law for the DL potential in terms of its length $\ell_{DL}$ and the electron density $n_{eK}$ on the low potential (cathode:K) side; we write this law as

$$\phi_{DL}(kV) \simeq 300 \left(\frac{n_{eK}}{10^2\ cm^{-3}}\right)\left(\frac{\ell_{DL}}{1\ km}\right)^2 , \qquad (1)$$

where $\ell_{DL} \equiv \phi_{DL}/\max|E_\parallel|$. In space, $\ell_{DL}$ is not limited a priori and, absent other constraints, equation (1) implies that the potential may grow to much larger values than the observed limit on the auroral precipitation energy, which is a few tens of keV.

This dilemma is resolved by considering how the field-aligned flanks of the arc become charged during the evolution of the DL's. We adopt as a starting point the basic idea of the recent MHD models discussed by Haerendel (1983) and Goertz (1985, 1986) in which the DL evolves in the parallel current sheet of a kinetic Alfvén wave. This scenario limits the thickness of the sheet a priori to a few times the ion gyroradius at an energy representative of the distant plasma population in the generator region. Taking this energy to be ~1 keV, we may estimate $j_\parallel$ by

$$j_\parallel = neU_{ei} \sim \frac{c}{4\pi}\frac{\delta B_\perp}{R_i}$$

Using $n \sim 10^2\ cm^3$, $B_0 \sim 0.05$ G, $\delta B_\perp \sim 10^{-3}$ G, and assuming a current sheet of a few kilometers thick, this equation gives a relative drift velocity $U_{ei}$ greater than the electron thermal velocity $V_e$. At such a relative drift velocity, the current sheet is unstable to a variety of instabilities, including the ion cyclotron and Buneman instabilities. We expect the instability to be triggered at some altitude $z_*$ where the density and magnetic field profiles first combine such that $U_{ei}$ exceeds the threshold drift. In addition, experiments reveal that the U-shaped structure, with the field-aligned flanks curved toward the low potential side as is required for Earthward-directed Poynting flux (Smith, 1986a), requires $\omega_e < \Omega_e$, where $\omega_e$ and $\Omega_e$ are the electron plasma frequency and gyrofrequency, respectively. This is just the condition for strong magnetization ($\omega_e/\Omega_e = R_e/\lambda_e$), and is fulfilled in a limited altitude range along the auroral field lines (Gurnett, 1974).

Simulations show that DL's evolve from current-driven instabilities when the current is interrupted by trapping (Smith, 1982a, b). Trapping creates local regions of macroscopic non-neutrality; in the finite-thickness current sheet, the plasma tends to expel charge in the transverse direction in an attempt to neutralize the local electric field (Fig. 1). Electrons are tightly magnetized and cannot be expelled very far, but the ion motion is essentially ballistic (the evolution time scale is $<\Omega_i^{-1}$), and ions are accelerated in the transverse direction out to some distance greater than their gyroradius. Owing to mirror forces, the expelled charge spreads upward, providing the initial charging of the flanks.

The charging mechanism described above operates in the transient phase. The characteristic time scale of the evolution is $\tau_{DL} \sim \ell_{DL}/U_{iA}$, where $U_{iA} > C_s$ the ion inflow velocity in the frame of the DL. The charge spreads along the flank at velocity $c/\sqrt{\epsilon_\perp}$, where $\epsilon_\perp$ is the dielectric constant. In the MHD limit, $\epsilon_\perp \simeq c^2/V_A^2$, but we shall see later that $\epsilon_\perp < c^2/V_A^2$ in the DL flank. In any case, however, we find that the time $\tau_{ind} = \int ds c/\sqrt{\epsilon_\perp}^{1/2}/c$ for the charge to spread along the field lines back to the generator region (Fig. 2) is long compared to $\tau_{DL} < t < \tau_{ind}$, the spreading

charge would thin out along **B** and the flank would not sustain the DL potential; then the DL would discharge. This would occur in a time short compared with the typical lifetime of discrete arcs. Therefore, asymptotic stability of the DA requires a transport mechanism producing a cross-field current density $J_x(\phi)$, which persists as $\partial\phi_{DL}/\partial t \to 0$.

If such a mechanism exists, then in the time-asymptotic regime, the density $n_{eK}$ in equation (1) is determined by current continuity and is of the form

$$n_{eK}(z_*) = n_{e\infty} - g \int_{z_*}^{\infty} dz\, J_x(\phi,z) \quad , \tag{2}$$

where g is a constant. Substituted in equation (1), equation (2) provides the physical constraint on the DL potential, which is transparently self-stabilizing for $J_x$, a monotonically increasing function of $\phi$.

A mechanism to maintain a distributed $J_x$ in the time-asymptotic regime is discussed by Smith (1986b). The mechanism is based on anomalous transport due to lower hybrid waves which are driven by the inhomogeneous structure of the flank itself. The discussion above implies that the initial scale length $\ell_f$ of the perpendicular electric field $E_x$ in the flank is $\ell_f > R_i$. As this field is established along **B**, the electrons acquire the local polarization drift velocity $cE_x/B_o$. The ions, however, encounter an inhomogeneous electric field over the scale of their gyroradius, and so their drift orbit is modified by finite-Larmor-radius (FLR) effects. For $\ell_f > R_i$, the ion drift speed is approximately given by the first non-vanishing order of the phase-averaged FLR correction:

$$V_{Di} \simeq (1 + \frac{1}{4} R_i^2 \nabla^2) \frac{cE_x}{B_o} \simeq \left(1 - \frac{R_i^2}{4\ell_f^2}\right) \frac{c\phi}{B_o \ell_f} \tag{3}$$

Then there is a relative drift

$$U_{ei} = V_{De} - V_{Di} \simeq \frac{R_i^2}{4\ell_f^2} \left(\frac{c\phi}{B_o \ell_f}\right) \quad ;$$

if $U_{ei} > V_i$, this relative drift drives the electrostatic modified two-stream instability (MTSI) studied by McBride et al. (1972). (Other instabilities are also possible, of course, but for simplicity we consider only the MTSI.) The most unstable mode has frequency $\omega \sim \omega_{LH} = \omega_i/(1 + \omega_e^2/\Omega_e^2)^{1/2}$, with growth rate $\gamma \sim \omega_{LH}$, and parallel wave number $k_\parallel \sim (m/M)^{1/2}\, k_\perp$.

The salient property of the MTSI for our purposes is that it saturates by trapping ions in the perpendicular drift direction and electrons in the parallel direction; in the saturation process, the ions and electrons are heated to a fraction $\alpha^2$ of the relative drift energy:

$$T_{\perp i} \simeq T_{\parallel e} \simeq \alpha^2 M U_{ei}^2/2 \; .$$

From simulations, McBride et al. (1972) find $\alpha \simeq 0.5$, with a wave energy density W at saturation of $W/nMU_{ei}^2 \sim$ a few percent.

Motivated by these results, Smith (1986b) postulates a self-scaling model in which the flank is assumed to be always at saturation (marginal instability) with respect to an instability such as the MTSI. The model characterizes the instability by two parameters $\alpha,\beta$, defined by

$$V_{\perp i} = \alpha\,(cE_x/B_o) \quad ; \quad U_{ei} = \beta\,(cE_x/B_o) \quad , \tag{4}$$

where $U_{ei}$ is now the threshold drift speed and $E_x \sim \phi/\ell_f$. Using equations (3) and (4), we find the self-similar scalings

$$R_i^2/\ell_f^2 = \alpha\beta \quad ; \quad T_{\perp i}/T_{eo} = (\alpha^3\beta)^{1/2}\,(e\phi_{DL}/T_{eo}) \quad ;$$

$$V_{De} \equiv \frac{cE_x}{B_o} = \left(\frac{\beta}{\alpha}\right)^{1/4}\left(\frac{m}{M}\right)^{1/2}\left(\frac{e\phi_{DL}}{T_{eo}}\right)^{1/2} \quad ; \qquad \left(\frac{\alpha}{\beta}\right)^{1/4}\left(\frac{M}{m}\right)^{1/2}\left(\frac{\omega_{eo}}{\Omega_{eo}}\right)\left(\frac{e\phi_{DL}}{T_{eo}}\right)^{1/2} \quad ; \tag{5}$$

where $\lambda_{eo}$, $T_{eo}$, and $\omega_{eo}$ are reference values of the electron Debye length, temperature, and plasma frequency.

Owing to momentum conservation, there is a wave-modulated friction between the electrons and ions, which may be described by an anomalous collision frequency (Davidson and Krall, 1977) $\nu_* \simeq \epsilon\omega_{LH}$, where $\epsilon \equiv W/nMU_{ei}^2$. Thus, the electron and ion fluids are acted on by volume forces $F_{yi} = -F_{ye}$, leading to an $\mathbf{F} \times \mathbf{B}$ drift velocity in the x-direction, i.e., opposite to $E_x$ (the coordinate system is defined by Fig. 3). This drift velocity is given by $V_{xe} = V_{xi} \equiv V_x\,(n_e,\phi_{DL})$, where

$$V_x = \epsilon\,(\alpha^3\beta^5)^{1/4}\left(\frac{m}{M}\right)^{1/2}\frac{\omega_{LH}}{\Omega_i}\left(\frac{e\phi_{DL}}{T_{eo}}\right)^{1/2} V_{eo} \quad , \tag{6}$$

and $V_{eo} = (T_{eo}/m)^{1/2}$. Thus, above the DL, plasma is transported from the center of the arc to the flanks, concentrating the parallel current there (Fig. 3). Although $V_{xe} = V_{xi}$, there is a net current $J_x$ because above the region of strong $E_\parallel$ in the DL, we expect an extended region of small charge density $\rho$ which sustains a weak parallel density field $E_\parallel$ driven by beam-plasma instabilities. Then the continuity equation is

$$\partial J_z/\partial z \simeq -\,\partial J_x/\partial x \approx -\,\partial(\rho V_x)/\partial x \quad ,$$

Upon solving and integrating along the field line, we obtain (Smith, 1986b)

$$J_z(\infty) - J_z(0) \simeq C(\alpha,\beta)\,(\phi_{DL}/\ell_a^2)^{5/8} \tag{7}$$

where $C(\alpha,\beta)$ is a constant and $\ell_a$ is the perpendicular scale length of the arc (Fig. 3). The RHS of equation (7) is just the term $\int J_x dz$ in equation (2). Assuming $J_z(0) << J_z(\infty)$, equation (7) gives a scaling law

$$\phi_{DL} \lesssim (J_z(\infty)/c)^{8/5}\, \ell_a^{\,2} \quad . \tag{8}$$

For typical auroral-zone parameters equation (8) yields $\phi_{DL} \sim 10$ kV for $\ell_a \sim 1$ km, in general accord with observations.

## III. SIMULATION

In the context of the above discussion, the flank may be modeled as a transmission line with local potential $\phi = E_x \ell_f$, where $\ell_f \sim \phi^{1/2}$. Once the DL potential has reached a threshold value $\phi_*$ required to drive the MTSI, the transmission line is charged by the distributed (in z) perpendicular current $J_x = \rho V_x$ of equation (7). We shall report elsewhere on simulations in which the transmission-line equations (Smith, 1986c) are solved simultaneously with a one-dimensional simulation of the DL evolution; this procedure provides the necessary self-consistent boundary condition on the current density $J_{DL}(t)$ at the simulation boundaries. In this paper, we replace the transmission line with a simple model circuit.

If the flank were uniform between the DL ($z = z_* \equiv 0$) and the generator, the transmission line would appear to the DL as a pure impedance over the evolution time of the DL, with value $Z_T = (L_T/C_T)^{1/2}$, where $L_T = \ell_f/4\pi c^2$, $C_T = 4\pi\epsilon_\perp/\ell_f$. We model the impedance by the same form, with variable $\ell_f(\phi)$. We thus adopt the model circuit shown in Figure 4 where the diode symbol represents the DL and the variable resistor $R(\phi)$ represents leakage current in the flank; this term is modeled by using the same form for $J_x$ as derived above, but over the perpendicular scale length $\ell_f$ instead of $\ell_a$, by integrating $J_x \sim n^{1/2}(z)$ over the length $z_K(t) = ct/\sqrt{\epsilon_\perp}$. The dielectric constant is defined by

$$\epsilon_\perp = 1 + (\omega_{eo}^2/\Omega_e^2) + (\omega_{io}^2/\Omega_i^2)\,[(1-\alpha\beta)^2 + \alpha^2(1+\gamma_e)] \quad , \tag{9}$$

where $\gamma_e \equiv T_{\|e}/T_{\perp i}$.

The heuristic definition [equation (9)] is such that the total energy stored in the dielectric is $\epsilon_\perp E_x^2/8\pi$: the first term in [] represents the reduced ion drift speed, while the second term accounts for ion and electron heating by saturation of the self-scaled modified two-stream instability.

For the purpose of testing the scaling of $\phi_{DL}$ with $\ell_a$ and $\alpha$, we adopt the philosophy that owing to the separation between the perpendicular scale lengths $\ell_a$ and $\ell_f$, the flank may be represented by these circuit elements while the DL will evolve in an essentially one-dimensional fashion in the central region of the arc. The DL evolution is simulated with the one-dimensional Vlasov code described by Smith (1982b), replacing the circuit used there by that of Figure 4. The boundary condition on the current density $J_{DL}(t)$ is then given by

$$J_{DL}(t) = \frac{I_S}{\ell_a} - \frac{\phi_{DL}(t)}{\ell_a}\left[\frac{1}{Z_T(\phi_{DL})} + \frac{1}{R(\phi_{DL})}\right] \quad , \tag{10}$$

where $I_S$ is the constant source current and

$$Z_T = [\alpha/\beta]^{1/4}\,(Y/\epsilon_\perp^{\,1/2})\,(V_{eo}/c)\,(\ell_a/\mu^{1/2})\,\phi_{DL}^{\,1/2} \quad , \tag{11}$$

$$R = \left(\frac{\mu}{2}\frac{T_{eo}}{T_{\|i}}\right)^{1/2} \frac{(Y\ell_a)^{2/3}}{(\alpha^7\beta)^{1/8}} \frac{\phi_{DL}{}^{1/4}}{[1-\exp(-K_2Z_K(t))/2]} \tag{12}$$

$\mu$ = m/M, $K_2$ is defined in Smith (1986b) $Y = \omega_{eo}/\Omega_{eo}$, $V_{eo} = \omega_{eo}\lambda_{eo}$, and all lengths and time scales are normalized to the nominal upstream quantities $\lambda_{eo}$ and $\omega_{eo}$, respectively; also $\phi_{DL} \to e\phi_{DL}/T_{eo}$. The term in [] in equation (10) replaces the physically derived $I_x$ of equation (8). This term is valid only after the threshold potential $\phi_*$ has been attained, and so is turned on adiabatically for $\phi > \phi_*$. Therefore, the circuit model does not accurately describe the initial dynamics in the linear instability phase of the evolution. In addition, the lumped circuit of Figure 4 cannot represent the distributed nature of the flank charging, and so we cannot construct a circuit topology that allows for inductive fields. Therefore, we cannot model the acceleration of the inflowing (injected) distributions by inductive effects.

For the parameters we use (see below), we estimate that the effect of neglecting inductive effects is small. As for the first limitation, the transient charging mechanism vanishes as $\partial\phi_{DL}/\partial t \to 0$. Thus, we expect the model to be adequate for our present objective of studying time-asymptotic scalings.

We show results for five runs. For all cases, the injected distributions are drifting Maxwellians with drift speeds in the simulation frame of $U_e = 2\,V_{eo}$, $U_i = -0.5\,V_{eo}$. The forms of these distributions are held fixed (up to normalization). The threshold drift parameter $\beta$ is held equal to 2, and M/m = 16. Holding $\ell_a/\lambda_e = 60$, we use values of $\alpha = 0.05, 0.02, 0.50$. Fixing $\alpha = 0.50$, we use $\ell_a/\lambda_e = 20, 40, 60$. Initialization and other implementations are as described by Smith (1982b).

Figure 5 shows the scaling of $\phi_{DL}$ with $\alpha$, the fundamental parameter of the self-scaling marginal stability model of the MTSI discussed earlier. In the circuit equation (10), the principal effect of $\alpha$ is contained in the dependence of the impedance $Z_T$ on the dielectric constant $\epsilon_\perp$. In terms of the circuit equation (10), the DL scaling law equation (1) becomes in dimensionless notation

$$\phi_{DL} = G\ell_{DL}{}^2J_s\left[1 - \frac{\phi_{DL}{}^{1/2}}{Z_oJ_s} - \frac{\phi_{DL}{}^{3/4}}{R_oJ_s}\right] , \tag{13}$$

where $Z_T(\phi) = Z_o\phi^{1/2}$, $R(\phi) = R_o\phi^{1/4}$. The RHS (13) has the form of a large factor $GJ_s\ell_{DL}{}^2$ times a small factor [...], and the upper bound for $\phi_{DL}$ is obtained from setting [...] = 0. Because $Z_o << R_o$, equation (13) implies $\phi_{DL} \sim Z_o{}^2$. In Figure 5 we also plot the dependence of $Z_o{}^2$ on $\alpha$, which agrees well with the plotted points.

Figure 6 confirms the scaling $\phi_{DL} \sim \ell_a{}^2$ found above. Again, this result is contained in equation (13) through the dependence $\phi_{DL} \sim Z_o{}^2$ (the results of Fig. 6 are all for $\alpha = 0.5$, where $Z_o << R_o$).

Because the speed of light c is introduced in the impedance, the choice of $V_{eo}/c$ yields a physical scaling of velocities. Because $Y = \omega_{eo}/\Omega_{eo}$ is a parameter, we obtain physical values of the length scales for an assumed value of either $B_o$ or $n_{eo}$. All runs discussed here are for $T_{eo} = T_{io} = 1$ keV, typical of the plasma sheet population (note $\phi_{DL}$ scales independently of $T_{eo}$). The scaled $\phi_{DL}$ is then given in kV as shown in the right-hand scale of Figure 6. Similarly, if we adopt a nominal value of $B_o = 0.05$ G ($f_{ce} = 250$ kHz) for the acceleration region, the top scale of Figure 6 gives arc thickness projected into the ionosphere of the order 1 km, which is the correct order of magnitude.

The power flows ($I\phi$) through the various parts of the circuit are shown for one case in Figure 7; for this case $\phi_{DL} = 42.5$ kV. In the steady state, only 10 percent of the power flows goes through the DL, and about 90 percent goes into charging the flanks. The physical scale on the right shows the power dissipated per 1000 km extent of the arc in the E-W direction. Arcs are generally observed in systems of parallel bands, quasi-periodic in the N-S direction; for the parameters of this example, each DA in such a system would dissipate about $10^{11}$ W, compared with a typical substorm power of $\sim 10^{12}$ W.

The scalings in $\alpha$ and $\ell_a$ have straightforward physical intepretations. The increase of $\phi_{DL}$ with $\alpha$ has two related aspects. First, the efficacy of the anomalous transport mechanism reported in Smith (1986b) increases with $\alpha$, which is a measure of the strength of the MTSI. Second, in this self-scaling model the ratio $R_i(\phi)/\ell_f(\phi) \sim \alpha^{1/2}$, so that as $\alpha$ increases, finite-Larmor radius effects lead to decreasing ion drift speed; hence, a higher ratio of electrostatic to kinetic energy is stored in the flank "dielectric" for a given charge. The factor $\ell_a$ in $Z_o$ [equation (6)] originates in the current balance ($I_s = J_s \ell_a$), and because the flank is charged from the interior of the arc the charge available increases with $\ell_a$. The quadratic scaling $\phi_{DL} \sim \ell_a^2$ derives from the self-scaling of the transport model because $\ell_f \sim \phi^{1/2}$.

## IV. DISCUSSION

We have shown that basic considerations of DL evolution and stability require anomalous transport processes to divert the uniform upstream current to the flanks of a DA even after the parallel electric field has evolved to a steady state. The transport model we have discussed, albeit highly simplified, yields an estimate [equation (8)] for the arc potential in general accord with observations. Other important consequences of the model are also in accord with satellite and rocket observations of DA's and laboratory DL experiments. These include: (1) the density in a DA is substantially depleted relative to the ambient density (Benson and Calvert, 1979; Alport et al., 1986); and (2) concomitant with the depletion of the arc is that the current is diverted to the flanks, so that the highest current density is at the edges (Bruning, 1983; Burke, 1984).

Besides the simple transport mechanism discussed here, there are many other mechanisms which are probably important in DA's. We are presently investigating models including ion-cyclotron modes.

In terms of the simple circuit model, the potentials, perpendicular length scales, and power flows physically scale to correct orders of magnitude. For the nominal parameters we have chosen, the potential ranges from 5 to 42 kV, while the length scales are consistent with the observational bound of $\simeq$3 km on the latitudinal scale projected in the ionosphere (Boehm and Mozer, 1981). These quantities scale as $n_{eo}$ and $n_{eo}^{-1/2}$, respectively. We adopted $B_o = 0.05$ to correspond to the frequency of peak intensity of the auroral kilometric radiation, and chose $\omega_{eo}/\Omega_{eo}$ as the marginal limit of strong magnetization ($\omega_e/\Omega_e = R_e/\lambda_e$), which experiments reveal to be a requisite for strong DL formation with Earthward-directed Poynting flux (Smith, 1986a). (Recall that $n_{eo}$ is the ambient density before DL formation, not that of the evacuated arc.) Thus, our choice of $\omega_{eo} = \Omega_{eo}$ is an upper bound; smaller values lead to lower potential, larger widths, and lower power flows.

In future publications we shall report on refinements and extensions of the simulation concept, including a model in which the simplified circuit used here is replaced by the transmission-line equations.

*Acknowledgments.* I am grateful to D. P. Chernin, A. T. Drobot, and C. K. Goertz for many stimulating conversations. I also thank J. B. McBride, C. L. Chang, W. Horton, J. D. Huba, A. Mankofsky, E. Ott, J. L. Seftor, and M. Temerin for useful discussions, and A. C. Williams for the invitation to present this work at the Workshop on Double Layers in Astrophysics. This work was supported by NASA contract NASW-3947.

## REFERENCES


Alport, M. J., S. L. Cartier, and R. L. Merlino, *J. Geophys. Res., 91,* 1599-1608 (1986).

Benson, R. F. and W. Calvert, *Geophys. Res. Lett., 6,* 479-482 (1979).

Boehm, M. H. and F. S. Mozer, *Geophys. Res. Lett., 8,* 607-610 (1981).

Bruning, K., Dissertation, Univ. of Munster, 1983.

Burke, W. J., in *Magnetospheric Currents,* edited by T. A. Potemra, Amer. Geophys. Union, Washington, D.C., pp. 294-303, 1984.

Coakley, P. and N. Hershkowitz, *Phys. Fluids, 22,* 1171-1181 (1979).

Davidson, R. C. and N. A. Krall, *Nuclear Fusion, 17,* 1313-1372 (1977).

Goertz, C. K., *Space Sci. Rev., 42,* 499-513 (1985).

Goertz, C. K., in *Comparative Study of Magnetospheric Systems,* edited by B. M. Pedersen, D. Le Queau, A. Roux, and A. Sant-Marc, CNRS, Toulouse, France, pp. 357-370, 1986.

Goertz, C. K. and G. Joyce, *Astrophys. Space Sci., 32,* 165-173 (1975).

Gurnett, D. A., *J. Geophys. Res., 79,* 4227-4238 (1974).

Haerendel, G., in *High-Latitude Space Plasma Physics,* edited by B. Hultqvist and T. Hagfors, Plenum, New York, pp. 515-535, 1983.

Kletzing, C., C. Cattell, F. S. Mozer, S.-I. Akasofu, and K. Makita, *J. Geophys. Res., 88,* 4105-4113 (1983).

McBride, J. B., E. Ott, J. P. Boris, and J. H. Orens, *Phys. Fluids, 15,* 2367-2383 (1972).

Smith, R. A., *Physica Scripta, 25,* 413-415 (1982a).

Smith, R. A., *Physica Scripta, T2,* 238-251 (1982b).

Smith, R. A., in *Unstable Current Systems and Plasma Instabilities in Astrophysics,* edited by M. R. Kundu and G. D. Holman, Reidel, Dordrecht, pp. 113-123, 1985.

Smith, R. A., in *Comparative Study of Magnetospheric Systems,* edited by B. M. Pedersen, D. Le Queau, A. Roux, and A. Saint-Marc, CNRS, Toulouse, France, pp. 327-350, 1986a.

Smith, R. A., *Geophys. Res. Lett.,* submitted, 1986b.

Smith, R. A., *Geophys. Res. Lett.,* submitted, 1986c.

Temerin, M., K. Cerny, W. Lotko, and F. S. Mozer, *Phys. Rev. Lett., 48,* 1175-1179 (1982).

Torbert, R. B. and F. S. Mozer, *Geophys. Res. Lett., 5,* 135-138 (1978).

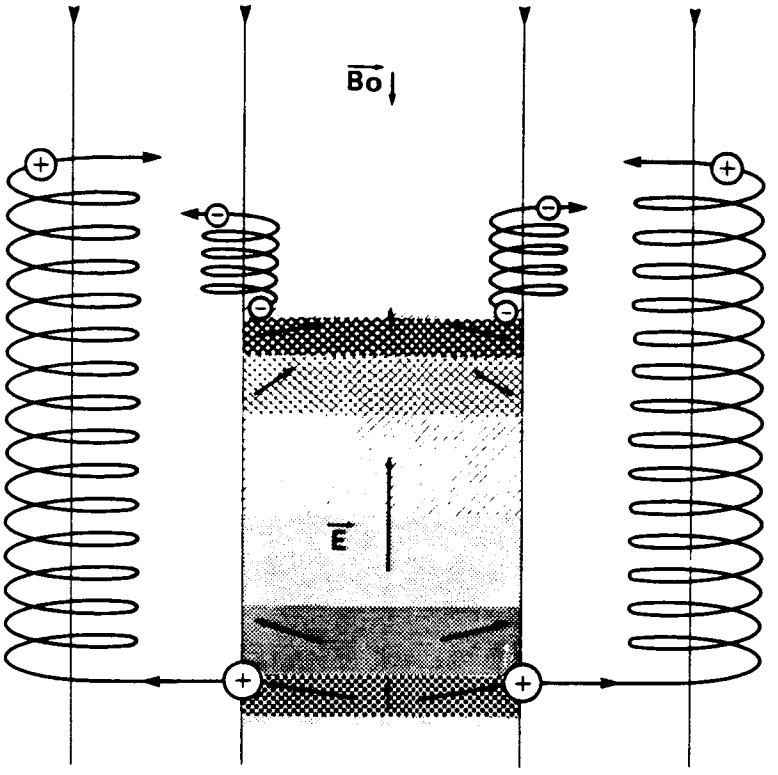


Figure 1. Schematic illustration of initial charging of the DL flanks by expulsion of charge from the localized, rapidly changing non-neutral region (shaded: stippled region $\rho > 0$, cross-hatched $\rho < 0$) where onset of current-driven instabilities occurs in the parallel sheet of a kinetic Alfvén wave.

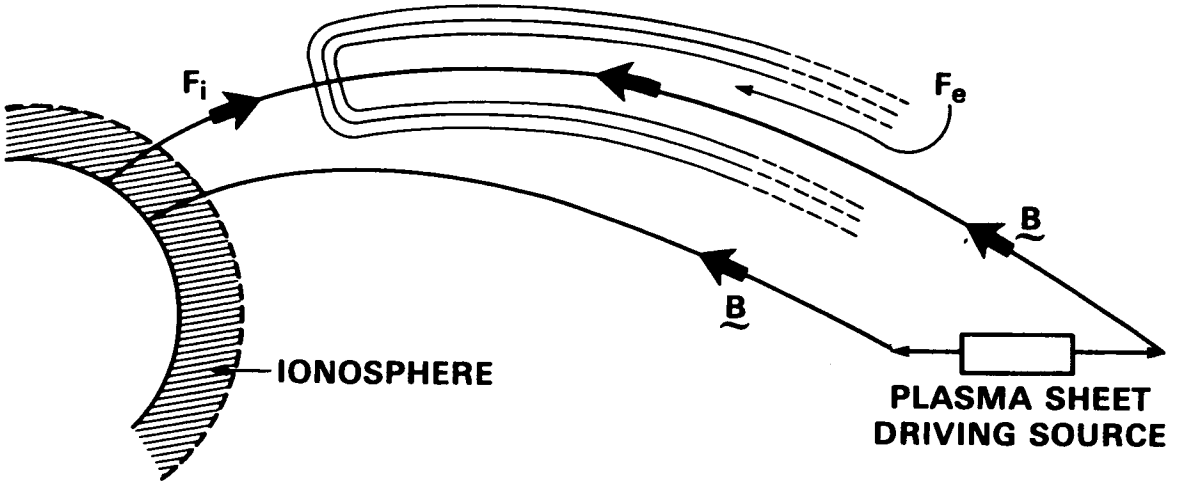


Figure 2. Schematic of the double layer flank spreading along **B** from the double layer toward the generator (here for illustration taken to be in the plasma sheet).

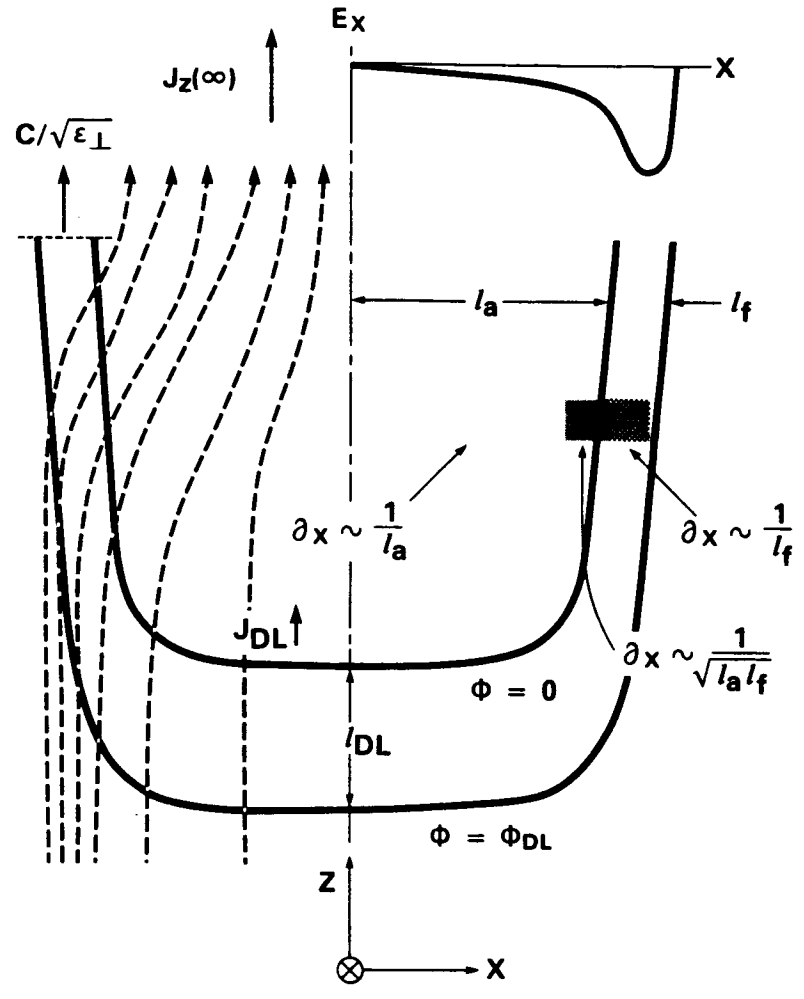


Figure 3. Left side: Schematic of the current diversion in the discrete arc. Right side: Definition of the scale lengths of the arc ($\ell_a$) and flank ($\ell_f$) and the associated scale factors which are used in the text to replace perpendicular derivatives. Also shown is a sketch of the inhomogeneous electric field $E_x$, which produces relative drift between the electrons and ions owing to finite-Larmor-radius effects, and the definition of the xyz coordinate system. The magnetic field $\mathbf{B}_o = -B_o e_z$.

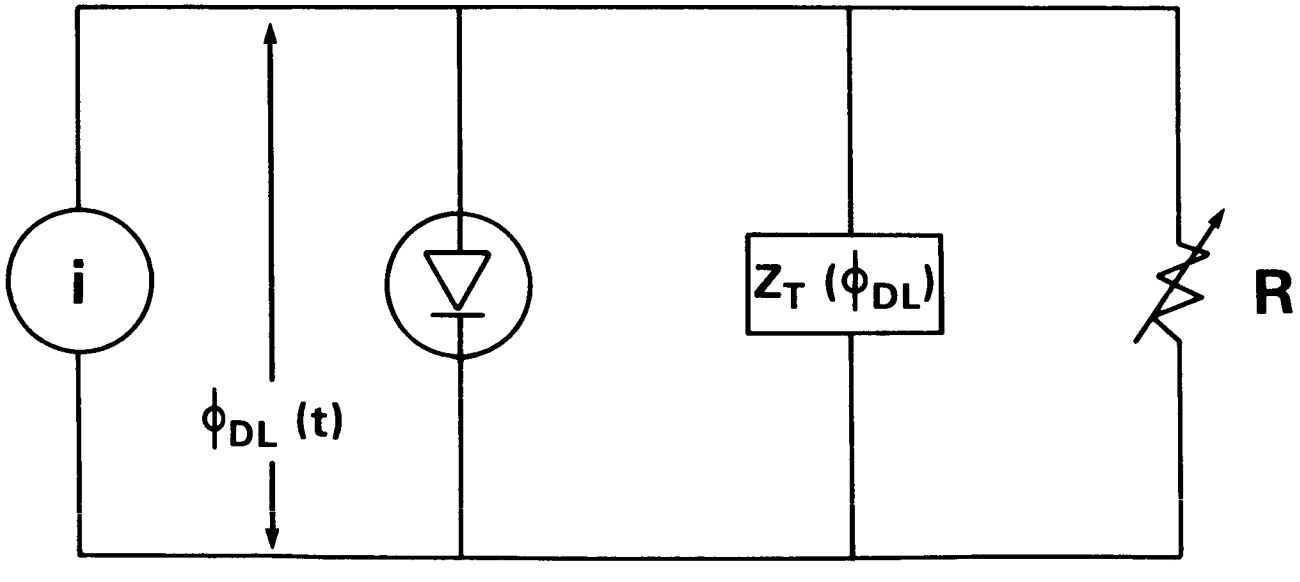


Figure 4. Model circuit used to provide the current density boundary condition in one-dimensional DL simulation.

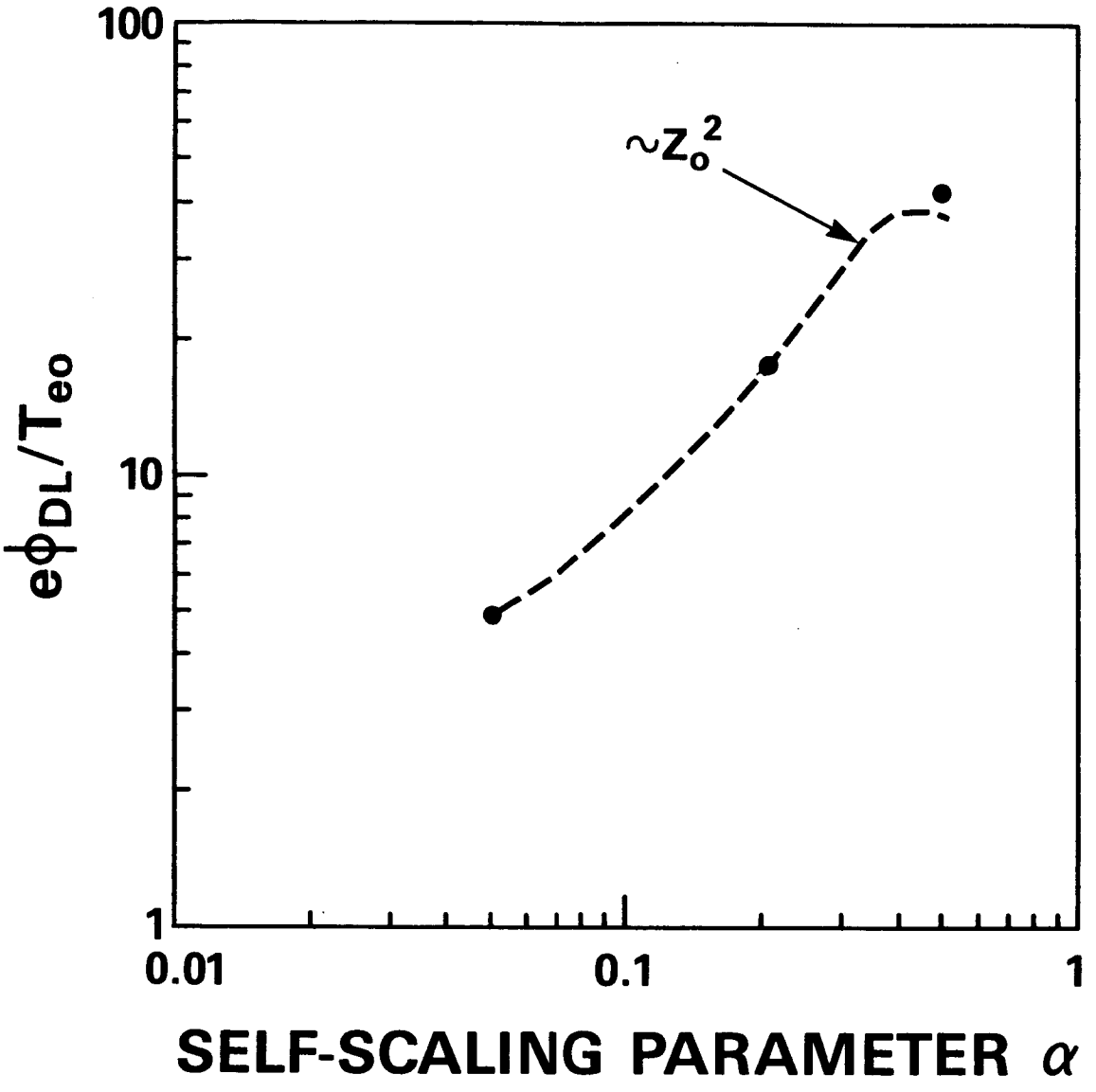


Figure 5. Scaling of the DL potential $\phi_{DL}$ with the fundamental parameter $\alpha$ of the anomalous transport mechanism. The dashed curve is arbitrarily normalized to the point at $\alpha = 0.2$.

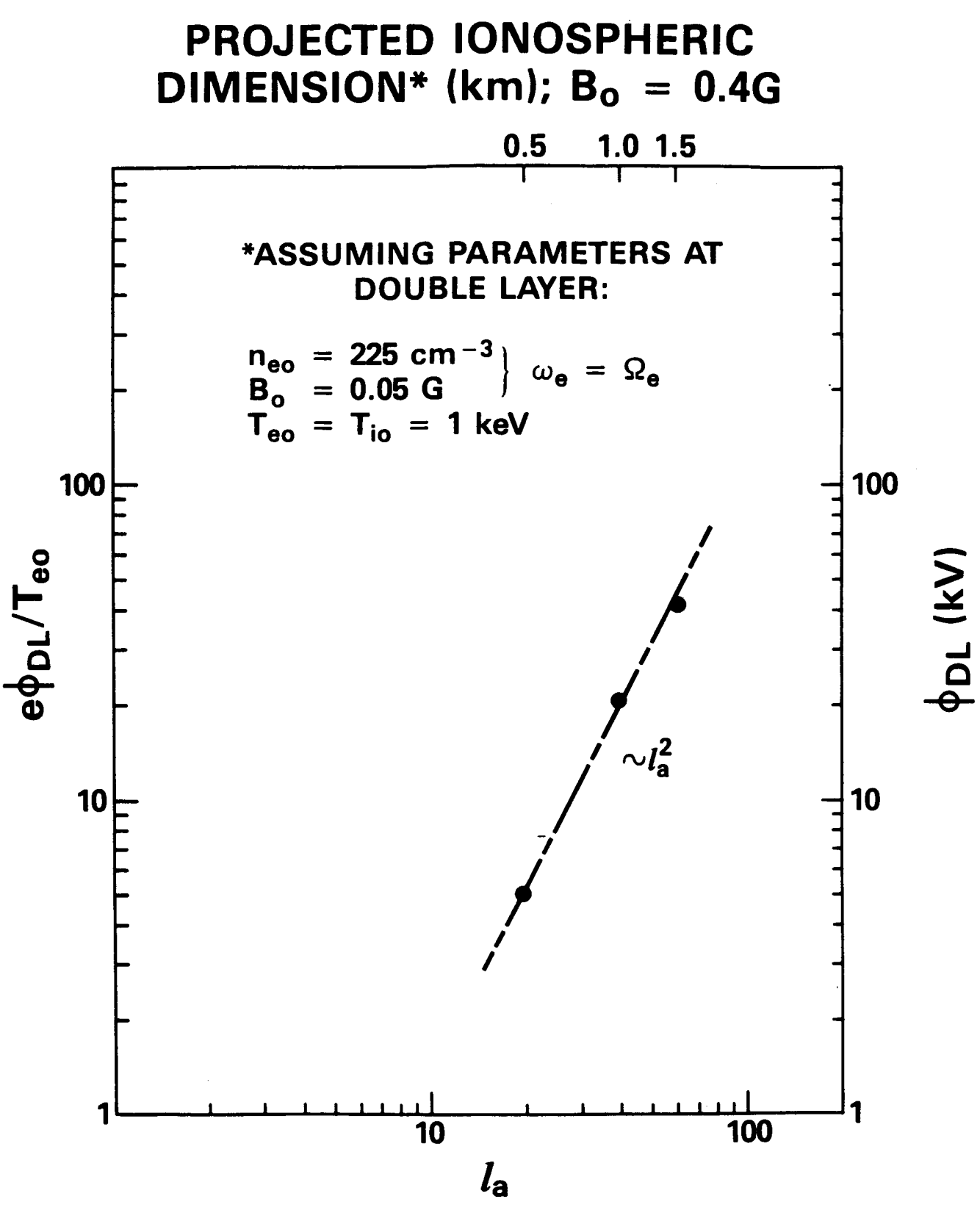


Figure 6. Scaling of $\phi_{DL}$ with the perpendicular scale width $\ell_a$ of the arc model. The bottom and left scales are dimensionless. The right scale shows the potential in kV for assumed $T_{eo}$ = 1 keV; the top scale shows the arc dimension ($2\ell_a$) projected into the ionosphere, for the given ambient parameters (before DL formation).

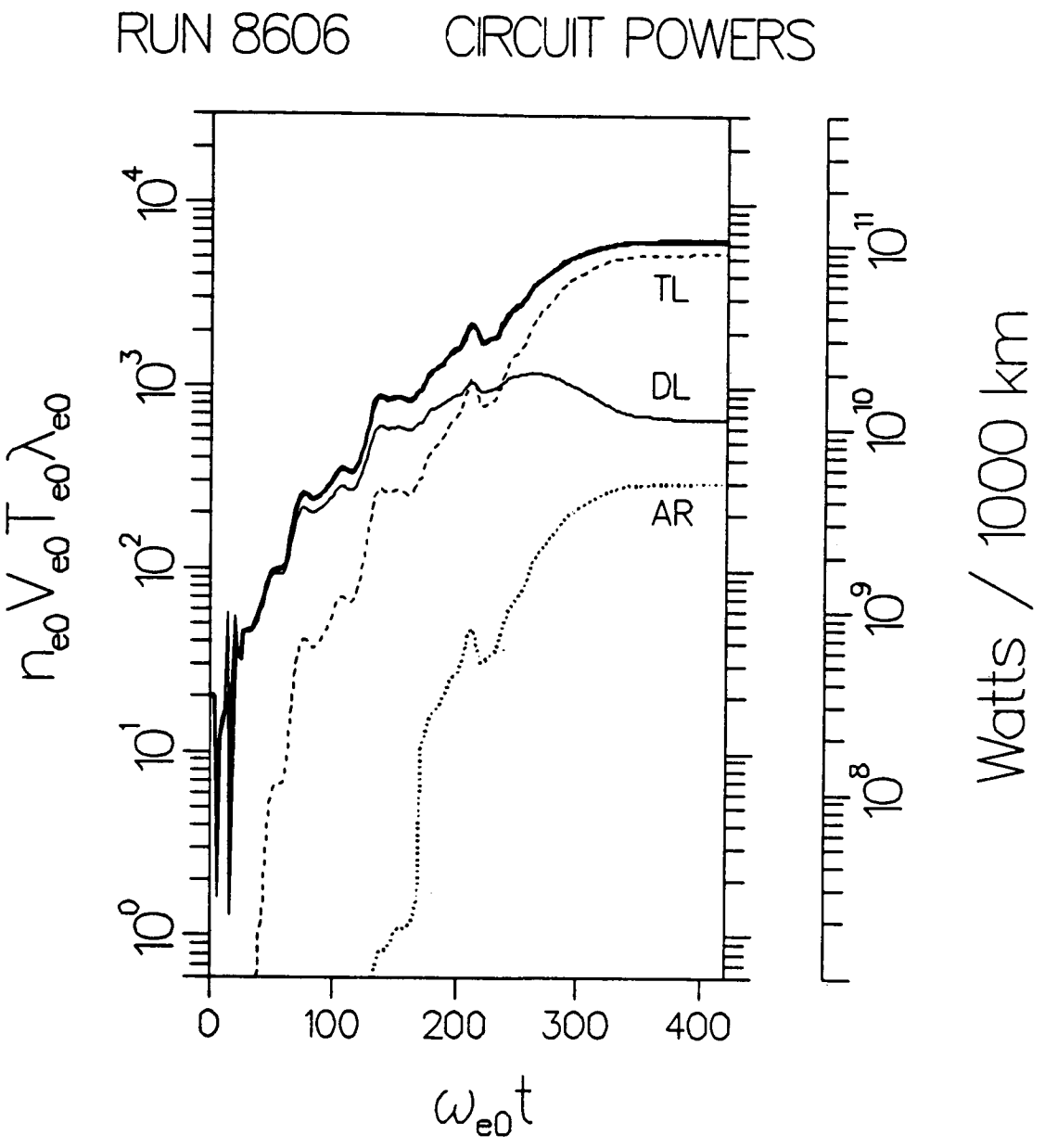


Figure 7. Time history of power flows through the various circuit elements for run 8606 ($e\phi_{DL}/T_{eo} = 42.5$). TL – transmission line (flank) impedance; DL – double layer; AR – anomalous resistivity (leakage) in flank. The right-hand scale shows the physically scaled power for an arc extended 1000 km in the E-W direction.